

KLF4 N-Terminal Variance Modulates Induced Reprogramming to Pluripotency

Shin-Il Kim,^{1,2} Fabian Oceguera-Yanez,¹ Ryoko Hirohata,¹ Sara Linker,^{1,3,6} Keisuke Okita,¹ Yasuhiro Yamada,^{1,2} Takuya Yamamoto,^{1,2} Shinya Yamanaka,^{1,2,4} and Knut Woltjen^{1,2,5,*}

¹Center for iPSC Cell Research and Application (CiRA), Kyoto University, Kyoto 606-8507, Japan

²Institute for Integrated Cell-Material Sciences (WPI-iCeMS), Kyoto University, Kyoto 606-8507, Japan

³John P. Hussman Institute for Human Genomics, University of Miami, Miami, FL 33136, USA

⁴Gladstone Institute of Cardiovascular Disease, San Francisco, CA 94158, USA

⁵Hakubi Center for Advanced Research, Kyoto University, Kyoto 606-8501, Japan

⁶Present address: Salk Institute for Biological Studies, La Jolla, CA 92037, USA

*Correspondence: woltjen@cira.kyoto-u.ac.jp

<http://dx.doi.org/10.1016/j.stemcr.2015.02.004>

This is an open access article under the CC BY-NC-ND license (<http://creativecommons.org/licenses/by-nc-nd/4.0/>).

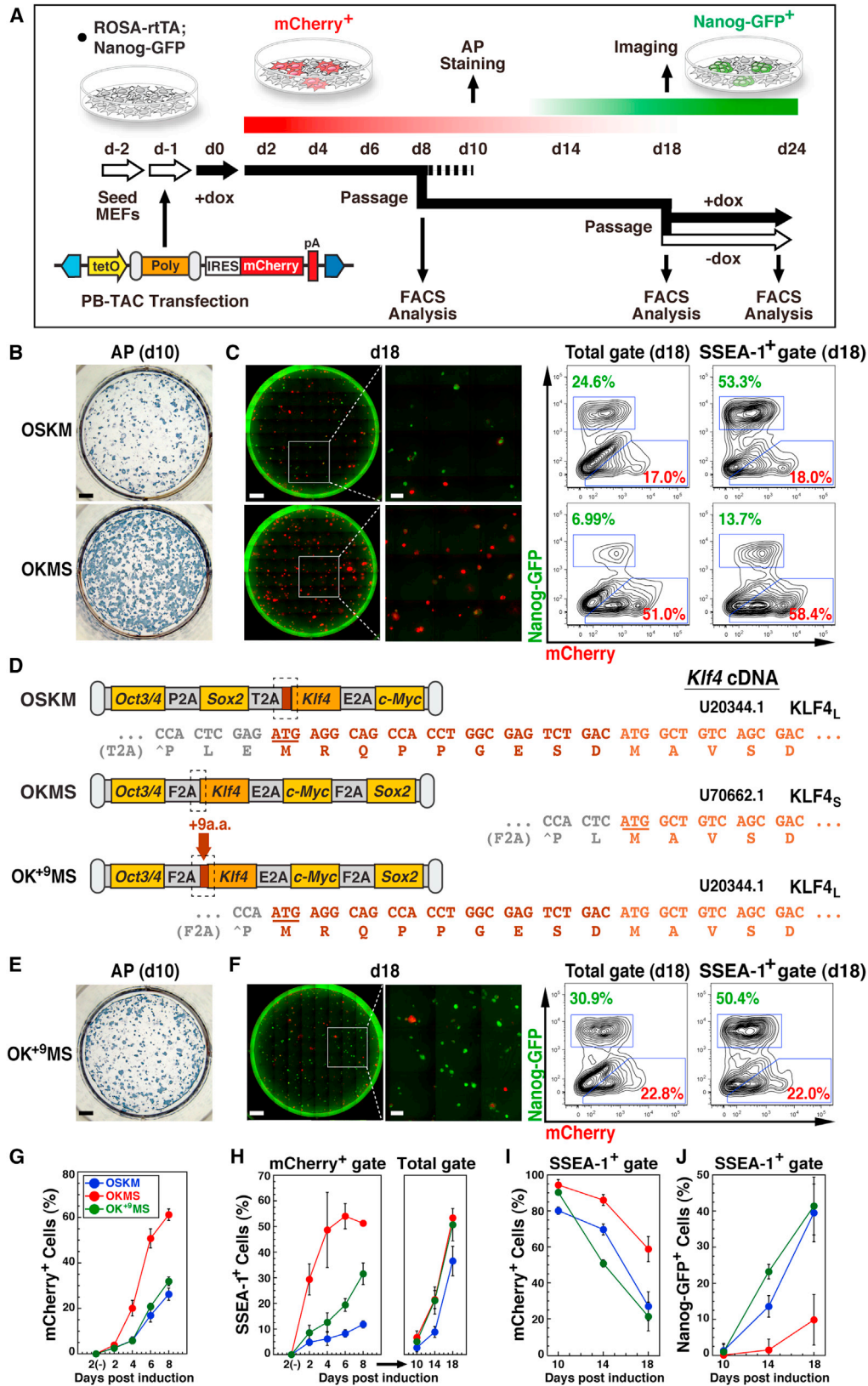
SUMMARY

As the quintessential reprogramming model, OCT3/4, SOX2, KLF4, and c-MYC re-wire somatic cells to achieve induced pluripotency. Yet, subtle differences in methodology confound comparative studies of reprogramming mechanisms. Employing transposons, we systematically assessed cellular and molecular hallmarks of mouse somatic cell reprogramming by various polycistronic cassettes. Reprogramming responses varied in the extent of initiation and stabilization of transgene-independent pluripotency. Notably, the cassettes employed one of two KLF4 variants, differing only by nine N-terminal amino acids, which generated dissimilar protein stoichiometry. Extending the shorter variant by nine N-terminal amino acids or augmenting stoichiometry by KLF4 supplementation rescued both protein levels and phenotypic disparities, implicating a threshold in determining reprogramming outcomes. Strikingly, global gene expression patterns elicited by published polycistronic cassettes diverged according to each KLF4 variant. Our data expose a *Klf4* reference cDNA variation that alters polycistronic factor stoichiometry, predicts reprogramming hallmarks, and guides comparison of compatible public data sets.

INTRODUCTION

Cellular identity can be guided by ectopic expression of master regulators (Graf, 2011). Deriving induced pluripotent stem cells (iPSCs) through the activities of OCT3/4, SOX2, KLF4, and c-MYC (Takahashi and Yamanaka, 2006) provides a potent model in which to study the role of transcription factor coordination in driving somatic cells toward pluripotency. Early mechanistic studies using mouse embryonic fibroblasts (MEFs) were conducted through de novo introduction of viral vectors, each expressing an individual (monocistronic) reprogramming factor (Brambrink et al., 2008; Stadtfeld et al., 2008a), where modulation of factor levels by viral titration led to altered reprogramming characteristics (Yamaguchi et al., 2011). Monocistronic reprogramming allows for variation in copy number and integration site, and as a result, stoichiometry is inconsistent on a cell-to-cell level. Therefore, this method was succeeded by the development of polycistronic factor cassettes that can produce multiple proteins from one single transcript (Kaji et al., 2009; Sommer et al., 2009). Although such fixed polycistronic stoichiometry revealed the importance of relative factor ratios in determining the quality of reprogramming (Carey et al., 2011), the principles that establish optimal stoichiometry remain undefined.

Studies of the mechanisms that underlie somatic cell reprogramming have revealed multi-step processes involving proliferation and cell-cell adhesion, along with molecular changes such as downregulation of lineage-specific genes and eventual upregulation of pluripotency markers (Plath and Lowry, 2011). Cell-surface markers were associated with reprogramming stages such as emergence of the embryonic stem cell (ESC) marker SSEA-1 (stage-specific embryonic antigen 1) (Polo et al., 2012; Stadtfeld et al., 2008a). Secondary reprogramming systems (Woltjen et al., 2009) helped define initiation, maturation, and stabilization as key stages in reprogramming toward pluripotency (David and Polo, 2014). Proliferation, colony formation, and a mesenchymal-to-epithelial transition (MET) define the initiation phase (Samavarchi-Tehrani et al., 2010), while stabilization is characterized by transgene independence and activation of pluripotency reporters such as *Nanog* and *Dppa4* (Golipour et al., 2012). Thus, changes in global gene expression and epigenetics were associated with the progression of reprogramming through these stages (Theunissen and Jaenisch, 2014). However, discrepancies in reprogramming platforms influence reprogramming hallmarks, the severity of MET responses, lineage-specific gene repression and ectopic activation, the timing of cell-surface marker presentation, and the frequency of partial and complete reprogramming (Golipour et al., 2012; Mikkelsen et al., 2008; O'Malley



(legend on next page)



et al., 2013; Polo et al., 2012; Samavarchi-Tehrani et al., 2010; Wernig et al., 2008).

In order to clarify such method-dependent reprogramming hallmarks, we applied standard assays to compare polycistronic cassettes (constructed in-house or obtained from public resources) in a drug-inducible *piggyBac* (PB) transposon reprogramming system. The induced expression of various polycistronic cassettes in mouse fibroblasts evoked phenotypic and gene expression changes that we divided into two basic behavioral classes. An examination of individual factor sequences across the panel of polycistronic constructs revealed a re-occurring discrepancy in the *Klf4* cDNA defining two coding region length variants. Increased length at the KLF4 N terminus was associated with higher protein levels and thus altered relative factor stoichiometry, ultimately impacting both the initiation and stabilization phases of iPSC derivation. Here, we report the consequences of KLF4 N-terminal variation in mono- and polycistronic reprogramming experiments, and apply these findings to recognize and reconcile differences in reprogramming characteristics implied hitherto.

RESULTS

A Transposon System for Collating Polycistronic Reprogramming Cassettes

Reprogramming studies in mouse have made use of unique polycistronic factor arrangements and delivery vectors. For uniform evaluation of factor-order effects, we employed

a fundamental reprogramming scheme based on factor transposition in MEFs (Woltjen et al., 2009). The PB transposon vector (PB-TAC) employs doxycycline (dox)-responsive reprogramming cassette expression co-incidentally with a mCherry reporter (Figure 1A). ROSA-rtTA; Nanog-GFP MEFs combine the m2-rtTA transactivator (Ohnishi et al., 2014) with a Nanog-GFP reporter (Okita et al., 2007). Thus, dox-responsive, PB-TAC-transgenic cells can be monitored throughout reprogramming initiation and maturation (day 2 [d2]–14) by mCherry fluorescence, while stabilization of pluripotency (d14–18) is indicated by activation of Nanog-GFP. Gain of factor independence through autonomous transgene silencing despite continued dox treatment is an established hallmark of the stabilization phase (Golipour et al., 2012), signaled here by a decrease in mCherry expression. For all polycistronic reprogramming cassettes tested, we routinely passaged populations on d8 and d18 using equal cell numbers without fractionation for extended culture and fluorescence-activated cell sorting (FACS) analysis. Dox-independent maintenance of iPSCs was verified by culture until d24, after which pluripotency was assayed by gene expression array and chimera contribution.

Initially, we used an alkaline phosphatase-positive (AP⁺) colony formation assay on d10 to compare various polycistronic cassettes with two previously published versions: OSKM (Carey et al., 2009) and MKOS (Kaji et al., 2009). Across the range of vectors tested, OKMS, constructed through the combination of OSKM and pCX-OKS-2A (Okita et al., 2008), displayed a reprogramming phenotype

Figure 1. KLF4 Isoforms Underlie Phenotypic Differences in Reprogramming

(A) Diagram of the PB reprogramming system and analysis steps. The PB-TAC transposon delivers inducible, reporter-linked (mCherry), polycistronic reprogramming cassettes (Poly) into ROSA-rtTA; Nanog-GFP MEFs (d-1). Cultures are induced with dox (d0, dox; filled arrows) and harvested on d8 for FACS and passage for late-stage analysis (d18). For AP staining, cultures are maintained without passage until d10. Full reprogramming and transgene independence is assessed by dox withdrawal from d18 to d24 (open arrows). Predicted expression periods for the mCherry and GFP reporters during iPSC derivation are shown with red and green gradated bars. Blue polygons represent PB 3' (left) and 5' (right) inverted terminal repeats. tetO, dox-responsive promoter; IRES, internal ribosome entry signal; pA, polyadenylation signal.

(B) AP staining on d10 of OSKM and OKMS reprogramming cultures. Scale bar, 4,000 μ m.

(C) Day 18 fluorescence microscopy of entire wells (composite 10 \times 10 fields) or selected insets (3 \times 3 subfields) for mCherry⁺ and Nanog-GFP⁺ (left). Scale bars, 4,000 μ m (full well) and 1,000 μ m (inset). FACS analysis of mCherry and Nanog-GFP expression in d18 Total and SSEA-1⁺ populations (right).

(D) Polycistronic cassette structure and sequence of the 2A-*Klf4* N-terminal cleavage junctions. Cloned cDNA is compared with murine *Klf4* GenBank mRNA sequences (U20344.1 and U70662.1), indicating the position of the predicted initiation codons and amino acid translations. The N-terminal 9aa of U20344.1 were introduced into OKMS (*Klf4_S*) to produce OK⁺MS (*Klf4_L*).

(E and F) The OK⁺MS construct was evaluated according to the assays outlined in (A)–(C). The results in (B), (C), (E), and (F) are representative of the results from at least three independent experiments (summarized in Figures S1A and S1B).

(G and H) Time-course analysis of mCherry⁺ cell expansion (G) and SSEA-1⁺ fractions (H) from OSKM, OKMS, and OK⁺MS transfections cultured for the indicated number of days before (2, 4, 6, 8) and after (10, 14, and 18) passage. Means \pm SE for three independent experiments.

(I and J) Time-course analysis of mCherry silencing (left) and Nanog-GFP activation (right) in SSEA-1⁺ cells on the indicated number of days after day 8 passage (10, 14, and 18). Means \pm SE for three independent experiments.

See also Figure S1.

contradictory to OSKM and MKOS (Figure 1B and data not shown). Despite similar transfection efficiencies (~3%–5% mCherry⁺ cells at d2 for both OSKM and OKMS), OKMS-induced AP⁺ colonies were clearly more abundant by d10, indicating that OKMS initiated somatic reprogramming more robustly than OSKM (Figures 1B and S1A).

To evaluate iPSC stabilization, we assayed activation of the Nanog-GFP pluripotency reporter and silencing of factor-linked mCherry after d8 passage of OSKM and OKMS reprogramming cultures. Whole-well microscopic evaluation revealed that most OKMS-induced colonies were unable to activate Nanog-GFP by d18 (Figure 1C, left), whereas mCherry expression remained high. In contrast, OSKM cultures showed a majority of GFP⁺ colonies with silenced mCherry. FACS on d18 confirmed the proportions of reporter-positive cells (Figure 1C, right). Both the Total GFP⁺ and SSEA-1⁺ GFP⁺ fractions on d18 were consistently higher for OSKM reprogramming (mean 15.6% and 39.5%, respectively, versus 5.4% and 9.9% for OKMS; Figure S1B). Conversely, overrepresentation of Total mCherry⁺ and SSEA-1⁺ mCherry⁺ populations was characteristic of OKMS (mean 53.1% and 58.8%, respectively, versus 21.0% and 27.0% for OSKM; Figure S1B). GFP⁺ cells emerged only in the SSEA-1⁺ fraction (data not shown), and only in mCherry^{low} or mCherry⁻ cells, such that double-positive GFP⁺ mCherry⁺ cells were not observed under either condition (Figure 1C, right). Reporter ratios remained mostly unchanged after d18 passage and an additional 6 days of culture in dox (d24; Figure S1C, left). Failure to activate Nanog-GFP was not associated exclusively with transgene interference, as dox withdrawal led to a complete loss of mCherry, but no increase in GFP for either the OSKM or OKMS populations (Figures S1C and S1D). For both vectors, dox-independent, Nanog-GFP⁺ iPSC clones contributed to chimera formation and clustered with ESCs in microarray transcriptome analyses, validating pluripotency (Figures S1E–S1G). These data suggest that OSKM more readily achieves stable reprogramming, whereas the majority of OKMS-induced cells remain in a transgene-dependent, partially reprogrammed state.

KLF4 Isoforms Underlie Phenotypic Differences in Polycistronic Cassette Reprogramming

We next sought to expose key differences underlying the distinct phenotypes observed for OSKM and OKMS, and initially examined the reprogramming factors at the DNA sequence level. Of particular interest, the 2A peptide cleavage site preceding *Klf4* in OSKM demarcated an ATG initiation codon that included an additional nine N-terminal amino acids (9aa) compared with that for OKMS (Figure 1D). When we examined public databases, we found that these two distinct *Klf4* isoforms correspond to open reading frames (ORFs) predicted from full-length

cDNA cloning (GenBank accession numbers U70662.1 and U20344.1) (Garrett-Sinha et al., 1996; Shields et al., 1996), anticipating proteins of 474aa and 483aa (GenBank accession numbers AAC52939.1 and AAC04892.1; henceforth referred to as KLF4_S and KLF4_L). To examine the effects of KLF4_S and KLF4_L on reprogramming while ruling out differences in factor order and 2A cleavage peptides, we introduced the N-terminal 9aa noted in OSKM (MRQPPGESD) directly into OKMS, producing OK⁺MS (where K⁺ is equivalent to KLF4_L).

MEFs transposed with OK⁺MS displayed a complete phenotypic switch. AP⁺ colony formation resembled that of OSKM (Figures 1E and S1A). Whole-well imaging on d18 strikingly revealed that OK⁺MS colonies were primarily GFP⁺ and there were few mCherry⁺ colonies (Figure 1F, left). The Total and SSEA-1⁺ fractions on d18 were predominantly GFP⁺ with extensive mCherry silencing, mirroring OSKM reprogramming behavior (Figures 1F, right, and S1B). Dox-independent, GFP⁺ OK⁺MS clones were chimera competent and shared a gene expression profile with OSKM and OKMS iPSCs, and ESCs (Figures S1E–S1G).

Extended FACS analysis revealed the kinetics of mCherry⁺ cell expansion throughout the early phase (d2–8), equating OK⁺MS with OSKM (Figure 1G). From our d8 FACS data, we found that a large proportion of OKMS mCherry⁺ cells were positive for SSEA-1. Therefore, we traced SSEA-1 dynamics from d2 to d8 (mCherry⁺ fraction; Figure 1H, left) and d10 to 18 post-passage (Total population; Figure 1H, right). Notably, only OKMS cultures were distinguished by rapid and robust SSEA-1 activation as early as d2 (29.4% versus 4.8% for OSKM, and 8.5% for OK⁺MS), which continued through early reprogramming. For all constructs, SSEA-1⁺ cells remained mCherry⁺ through d8, at which point no Nanog-GFP activation could be detected. An examination of the increasing proportion of SSEA-1⁺ cells over d10–18 (Figure 1H, right) showed that activation of Nanog-GFP and coincident suppression of mCherry by OK⁺MS were more consistent with OSKM, whereas for OKMS, both mCherry silencing and Nanog-GFP activation were less frequent (Figures 1I and 1J). Overall, these data indicate that elongation of *Klf4*_S to *Klf4*_L in OK⁺MS subdues early reprogramming hallmarks but positively regulates stabilization of pluripotency.

Monocistronic Expression of *Klf4*_S or *Klf4*_L Does Not Differentially Influence Reprogramming

To determine whether the observed cassette-specific phenotypes were due to functional differences between KLF4_S and KLF4_L, we performed a series of monocistronic *Klf4* expression experiments. We found that the transcriptome profiles of d6 mCherry⁺ cells arising from PB-TAC-*Klf4*_S or -*Klf4*_L MEF transfections were highly correlated (R = 0.999; Figure S2A). Gene enrichment compared with



mock-transfected MEFs revealed a common set of 476 genes enriched for Gene Ontology (GO) terms associated with extracellular matrix, skin development, and cell adhesion (Figure S2B). Activation of a KLF4-responsive *Lefty1*-luciferase reporter (Nakatake et al., 2006) was similar irrespective of the KLF4 variant (Figure S2C), indicating that the capacity for regulation of this ESC promoter was unchanged. Moreover, both KLF4_S and KLF4_L could similarly rescue leukemia inhibitory factor (LIF)-independent culture of 1A2 Nanog-GFP reporter ESCs (data not shown). Thus, independent expression of either *Klf4* variant supported a preservation of functional capacity.

Considering the remarkable reprogramming phenotypes observed with polycistronic cassettes, we next addressed whether monocistronic expression of *Klf4*_S or *Klf4*_L in combination with polycistronic *Oct3/4*, *Sox2*, and *c-Myc* (OMS) had any detectable effect on iPSC derivation. OMS alone did not foster expansion of mCherry⁺ cells, which remained at a steady ~6% through d18, nor did it activate SSEA-1 or Nanog-GFP expression (data not shown). Interestingly, expression of either *Klf4* variant in combination with OMS resulted in nearly indistinguishable reprogramming phenotypes using the assays outlined in Figure 1 (see also Figures 2A, S2D, and S2E). These data demonstrate that the phenotypes associated with KLF4_S and KLF4_L arise mainly in the context of polycistronic factor linkage.

KLF4 Levels Are Diminished in OKMS and Rescued by N-Terminal Elongation

In order to rationalize the phenotypic differences observed between polycistronic cassettes, we evaluated transgene expression at the transcriptional and translational levels. Quantification of polycistronic mRNA revealed similar expression levels for OSKM and OKMS (Figure S2F). Strikingly, western blotting on d2 revealed that dox-induced KLF4 was expressed at distinctly higher levels in OSKM compared with OKMS, whereas the levels of OCT3/4, SOX2, and c-MYC were generally comparable (Figure 2B). High KLF4 stoichiometry was also observed in MKOS, which, like OSKM, encodes KLF4_L (Figure S2G). Consistent with the PB transposon experiments, MEFs from gene-targeted *Col1a1*-OSKM (Ohnishi et al., 2014) and -OKMS ESC chimeras faithfully reproduced cassette-specific protein levels (data not shown). Moreover, OK⁺MS resulted in a marked increase in KLF4 levels compared with OKMS (Figure S2H). Surprisingly, N-terminal elongation of KLF4_S in OKMS with a hemagglutinin (HA) epitope also rescued protein levels (OK_{N-HA}MS; Figure S2H) and even reprogramming phenotypes (Figure S2I), whereas N-terminal HA extension of KLF4_L in OK⁺MS did not result in any additional phenotypic change. Concordant with monocistronic phenotypes, transfection of PB-TAC-

*Klf4*_S or -*Klf4*_L in MEFs produced comparable protein levels on d2 (Figure S2J). These data indicate that the protein sequence at the KLF4 N terminus plays a role in specifically establishing polycistronic factor stoichiometry.

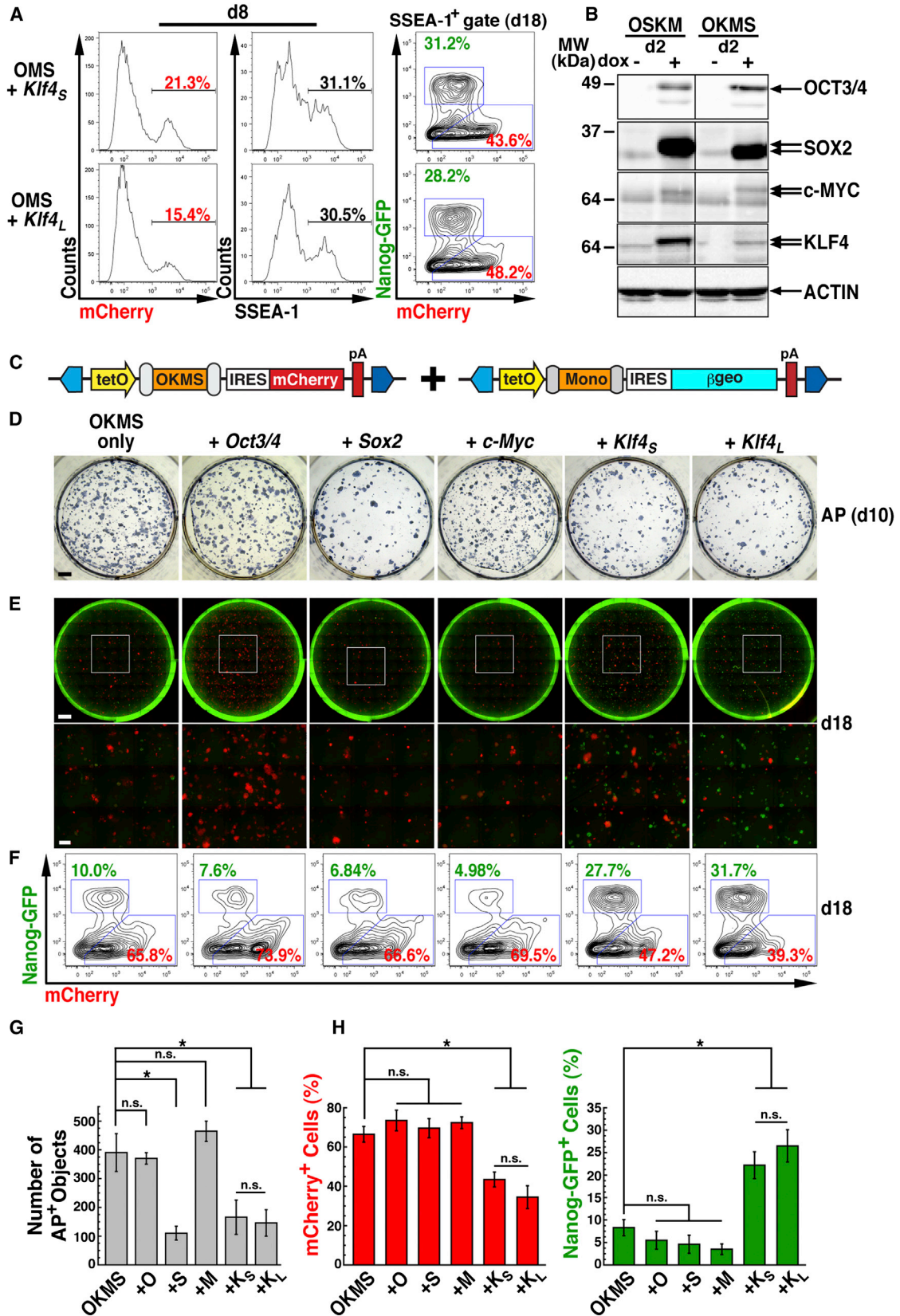
KLF4 Stoichiometry Regulates Reprogramming

To verify the reprogramming outcomes from adjusted factor stoichiometry, we supplemented OKMS with monocistronic factors in a PB-TAB transposon (Figure 2C). Supplementation of OKMS with *Klf4*_S or *Klf4*_L (Figure S2J) markedly reduced d10 AP⁺ colony numbers (Figures 2D and 2G), reminiscent of the reduced colony formation efficiencies observed when OSKM or OK⁺MS was employed. *Sox2*, but not *Oct3/4* or *c-Myc*, also had a significant effect on reducing colony formation frequencies compared with OKMS alone. Thus, both KLF4 isoforms modulated OKMS factor stoichiometry to subdue reprogramming initiation.

In the late phase of reprogramming, we gauged stabilization via mCherry silencing and Nanog-GFP activation (Figures 2E, 2F, and 2H). Supplementation of OKMS with either *Klf4*_S or *Klf4*_L was capable of activating Nanog-GFP with co-incident repression of mCherry on d18. Interestingly, although *Sox2* supplementation also showed a repressive effect on initiation, d18 mCherry⁺ and GFP⁺ proportions remained mostly unchanged, indicating that additional *Sox2* fails to rescue the OKMS stabilization phase. Likewise, *Oct3/4* and *c-Myc* failed to promote Nanog-GFP reporter activation or mCherry silencing. Thus, only *Klf4* variants were capable of augmenting the OKMS phenotype, implying a sensitivity of reprogramming pathways to KLF4 expression thresholds.

KLF4 Stoichiometry Is Reflected in Gene Expression Analyses

Global gene expression has been used to define reprogramming paths. In order to link gene expression to initial reprogramming behaviors, we subjected d6 mCherry⁺ cells from PB-TAC-OSKM, -OKMS, -OK⁺MS, and -MKOS to microarray analysis (Figures 3A and 3B). Based on OSKM and OKMS GO term enrichment (data not shown) and results from previous reports, we established sample indexing criteria (Figure 3A, left). *Krt14* and *Krt17* (encoding structural proteins), as well as *Sfn* (a regulator of epithelial cell growth), are claimed to activate in reprogramming populations with preferred iPSC fate (O'Malley et al., 2013). Expression of *Ocln* and *Cdh1* indicates MET responses (Samavarchi-Tehrani et al., 2010), while additional cell-surface changes are reflected by upregulation of *Cadm1* and *Fut9* (the fucosyltransferase responsible for producing SSEA-1). The developmental regulators *Tbx21* and *Bcl11a* (transiently upregulated non-ESC markers; Polo et al., 2012) and the pre-iPSC marker *NrOb1* (Mikkelsen et al.,



(legend on next page)



2008) show the extent of reprogramming. As early as d6, these ten marker genes were >2-fold differentially expressed between OK⁺MS (green series) and OKMS (red series; Figure 3A, left), and <2-fold differentially expressed in a pairwise correlation of OSKM to OK⁺MS (R = 0.993; Figure 3A, top right), certifying our indexing for further pairwise comparisons. Correlation and indexing of OSKM to OKMS verified the influence of KLF4 on early gene expression responses (Figure 3A, bottom right).

GO term analysis of commonly upregulated gene expression versus mock-transfected MEFs (PB-TAC-lacZ) was performed for cassettes containing *Klf4_L* and *Klf4_S* (Figure 3B and data not shown). For *Klf4_S* vectors (216 genes), only a few GO terms related to the biological processes “regulation of cell adhesion (laminins)” and “tissue morphogenesis,” as well as the molecular function of “phospholipase C activity,” were enriched with p values ≤ 1.0E-3 (data not shown). Nearly double the number of genes were activated by *Klf4_L* constructs (512 genes; Figure 3B; Table S1). The common gene set for polycistronic *Klf4_L* constructs significantly enriched GO terms for cellular components of the “plasma membrane” and “cell-cell junction” (consistent with an expected MET response), as well as distinct enrichment for “keratinocyte differentiation” and “epidermal cell differentiation” biological processes (p = 2.3E-11 and 5.4E-11; Figure 3B, right) with Benjamini scores = 3.6E-8 and 4.1E-8, respectively. These data are consistent with monocistronic *Klf4* expression (Figure S2B).

KLF4 Isoforms Divide Reprogramming Cassettes into Two Major Classes

In order to more broadly understand the impact of KLF4-mediated reprogramming outcomes, we extended our

analysis of publically available polycistronic constructs. DNA sequence surveys revealed that *Klf4_S* and *Klf4_L* reference cDNAs have been used interchangeably in the reprogramming field (Table 1). To confirm that public polycistronic vectors also display incongruous reprogramming behaviors, we selected MKOS (Kaji et al., 2009), STEMCCA (Sommer et al., 2009), EB-C5 (Chou et al., 2011), and WTSI (Yusa et al., 2009), and applied our battery of phenotyping tests (Figure S3). mCherry⁺ fractions and AP⁺ colony numbers varied among cassettes but were highest for OKMS and EB-C5 (Figures S3A and S3C). Notably, all four *Klf4_S* cassettes (OKMS, STEMCCA, EB-C5, and WTSI) showed large proportions of mCherry⁺ SSEA-1⁺ cells on d8 (>40%, compared with <21% for *Klf4_L* cassettes OSKM, OK⁺MS, and MKOS; Figure S3B), a characteristic that was consistently associated with *Klf4_S* (Figure 1H). In accordance with *Klf4_L* construction and western blotting data (Figure S2G), MKOS AP⁺ colony numbers were low on d10, and became mostly GFP⁺ mCherry⁻ colonies on d18 (Figures S3D and S3E). On the other hand, the *Klf4_S* cassettes STEMCCA, EB-C5, and WTSI all perpetuated mCherry expression after d8 passage (74.8%, 80.9%, and 79.6%, respectively), and activated Nanog-GFP in <3.0% of SSEA-1⁺ cells (Figure S3E). Thus, the phenotypes elicited by these additional public cassettes predictably correlated reprogramming hallmarks with *Klf4* coding length.

Finally, gene indexing confirmed that MKOS (*Klf4_L*) is distinct from STEMCCA (*Klf4_S*; Figure 3C), substantiating the phenotypes reported in Figure S3. Moreover, unsupervised clustering of d6 mCherry⁺ cell gene expression profiles from all eight constructs (PB-TAC-OSKM, -OKMS, -OK⁺MS, -OK_{N-HA}MS, -MKOS, -STEMCCA, -EB-C5, and -WTSI) generated a dendrogram (Figure 3D) that distinctly

Figure 2. KLF4 Stoichiometry Affects Reprogramming Phenotypes

(A) Reprogramming with polycistronic OMS + monocistronic *Klf4_S* or *Klf4_L* leads to nearly identical phenotypes, as analyzed by FACS for mCherry or SSEA-1 on d8 (left) and mCherry versus Nanog-GFP on d18 (right).

(B) Western blot analysis of OCT3/4, SOX2, c-MYC, and KLF4 in OSKM or OKMS transfected MEFs cultured for 2 days with or without dox treatment. Actin was used as a loading control. Arrows show the two KLF4 isoforms. Note that SOX2 and c-MYC also differ in size based on their positions relative to 2A peptides in the polycistronic cassette (Figure 1D). Uncropped data are provided in Figure S2G.

(C–F) Supplementation of PB-TAC-OKMS was performed by co-transfection of additional factors in PB-TAB transposons. β-geo, lacZ-neo fusion gene.

(D) AP staining on d10 after transfection with OKMS alone or in combination with *Oct3/4*, *Sox2*, *c-Myc*, *Klf4_S*, or *Klf4_L*. Scale bar, 4,000 μm.

(E) Day 18 fluorescence microscopy of entire wells (composite 10 × 10 fields) or selected insets (3 × 3 subfields) for mCherry⁺ and Nanog-GFP⁺. Scale bars, 4,000 μm (full well) and 1,000 μm (inset).

(F) FACS analysis of mCherry and Nanog-GFP fractions in the d18 SSEA-1⁺ population of the cultures shown in (E). The results in (D)–(F) are representative of the results of at least three independent experiments (summarized in G and H).

(G) Quantification of the effects of factor supplementation on AP⁺ colony formation (D). Means ± SE for three independent experiments. n.s., not significant. *p < 0.05, Student's t test.

(H) Percentages of mCherry⁺ and Nanog-GFP⁺ populations from FACS analysis of factor supplementation (F). Means ± SE for three independent experiments. n.s., not significant. *p < 0.05, Student's t test.

See also Figure S2.

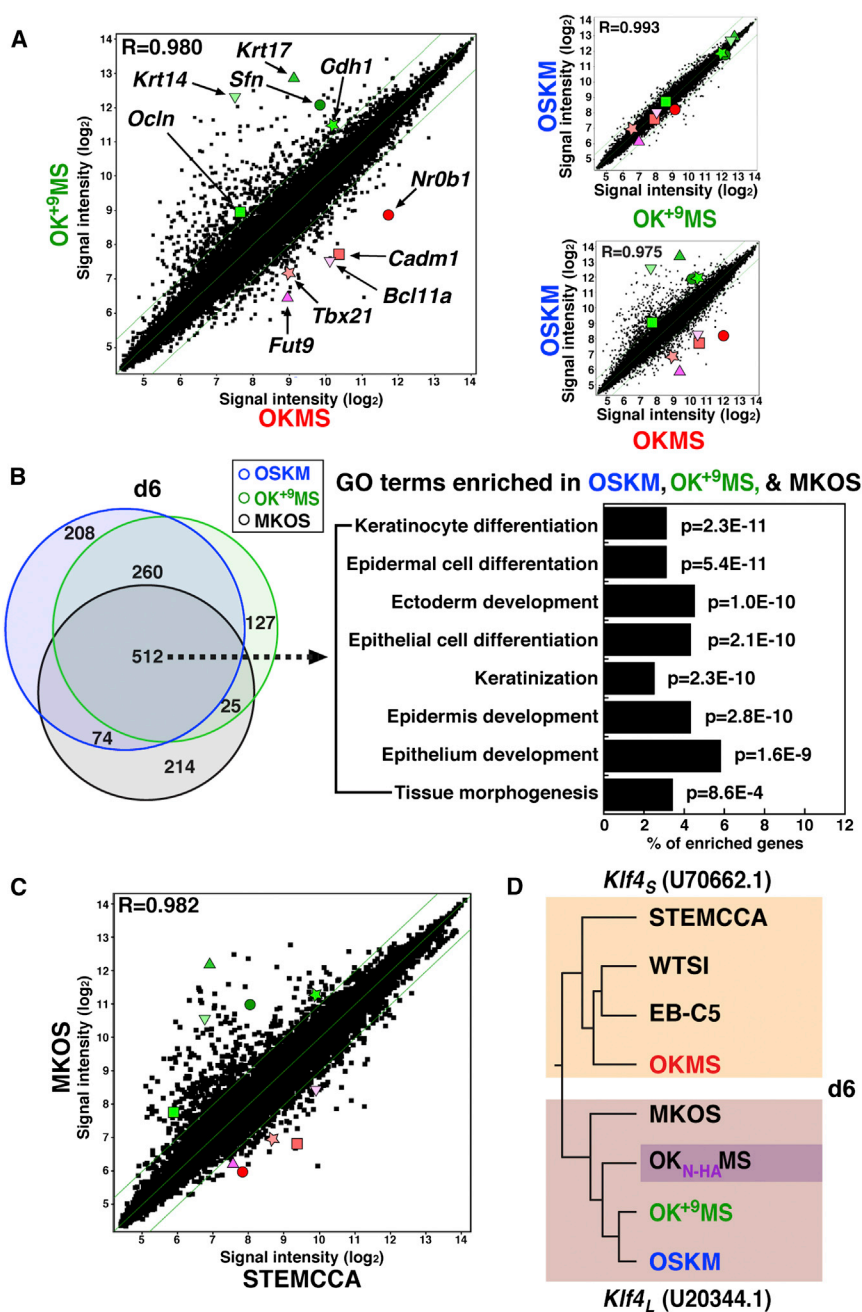


Figure 3. Gene Expression Patterns Reveal *Klf4* Variants

(A) Pairwise comparison of global gene expression in mCherry-positive cells on d6 from OSKM, OKMS, and OK⁺⁹MS reprogramming. Diagonal lines indicate 2-fold changes in log₂ signal intensity. Genes chosen for indexing are highlighted. Green: *Krt17*, triangle; *Sfn*, circle; *Ocln*, square; *Gdh1*, star; *Krt14*, inverted triangle. Red: *Fut9*, triangle; *Nr0b1*, circle; *Cadm1*, square; *Tbx21*, star; *Bcl11a*, inverted triangle.

(B) Left: Venn diagram showing overlapping gene activation versus lacZ-MEFs in the *Klf4_L* cluster. Right: GO analysis of 512 shared d6 genes, arranged in order of p value and indicating the proportion of genes represented for each enriched GO term. Cutoff $p = 1.0E-3$.

(C) Pairwise comparison of global gene expression in mCherry-positive cells on d6 from MKOS and STEMCCA reprogramming. Highlighted genes are those indicated in (A).

(D) Dendrogram resulting from unsupervised clustering of OSKM, OKMS, OK⁺⁹MS, OK_{N-HA}MS, MKOS, STEMCCA, EB-C5, and WTSI mCherry d6 array samples. Segregation of the vectors based on the nature of the KLF4 N terminus is indicated. See also Figure S3 and Table S1.

bifurcated based on the *Klf4* variant employed in each vector (Table 1). Thus, early gene expression patterns disclosed the nature of cloned *Klf4*. Intriguingly, despite unrelated N-terminal sequence identity (yet predicted by phenotype), OK_{N-HA}MS activated 463/512 (~90%) of the core *Klf4_L* genes (data not shown) and clustered with *Klf4_L* vectors (Figure 3D). A standardized comparison of polycistronic reprogramming cassettes thus implicates KLF4 isoforms in differential modulation of the reprogramming transcriptome.

DISCUSSION

Principally, we have uncovered a fundamental characteristic of cloned *Klf4* that governs relative factor stoichiometry and reprogramming responses during mouse iPSC derivation with polycistronic constructs. At the root of our discovery lies the disparate coding prediction of full-length *Klf4* cDNA (Garrett-Sinha et al., 1996; Shields et al., 1996), resulting in two proteins with distinct N termini defined herein as KLF4_S and KLF4_L. These two

Table 1. Survey of Publicly Available Reprogramming Cassettes

Source				Construct Data				Form ^e		Sequence Validation			Publication	
Distribution ^a	Addgene Collection ^b	Depositing Scientist	Repository ID	Plasmid Name	Gene/Insert Name	Species ^c	Type ^d	Klf4 _S	Klf4 _L	AddGene ^f	Depositor	Direct ^g	PMID	Reference
Addgene	stem cell; Klf4/KLF4	Shinya Yamanaka	13370	pMXs-Klf4	Kruppel-like factor 4 (gut)	<i>M. musculus</i>	mono	●	—	○	○	○	16904174	Takahashi and Yamanaka, 2006
Addgene	stem cell; Klf4/KLF4	Shinya Yamanaka	15920	pMXs-Klf4-IP	Kruppel-like factor 4 (gut)	<i>M. musculus</i>	mono	●	—	○	○	○	16904174	Takahashi and Yamanaka, 2006
Addgene	Klf4/KLF4	Miguel Ramalho-Santos	15950	pLOVE-Klf4	Kruppel-like factor 4	<i>M. musculus</i>	mono	n/d	n/d	n/c	—	—	18371358	Blelloch et al., 2007
Addgene	stem cell; Klf4/KLF4	Shinya Yamanaka	17219	pMXs-hKLF4	KLF4	<i>H. sapiens</i>	mono	●	—	○	○	○	18035408	Takahashi et al., 2007
Addgene	stem cell; Klf4/KLF4	George Daley	17227	pMIG-hKLF4	Kruppel-like factor 4 (gut)	<i>H. sapiens</i>	mono	●	○	○	—	—	18157115	Park et al., 2008
Addgene	stem cell; Klf4/KLF4	Kathrin Plath	17967	pMXs-hKLF4 (Plath)	Kruppel-like factor 4 (gut)	<i>H. sapiens</i>	mono	●	○	○	○	—	18287077	Lowry et al., 2008
Addgene	stem cell; Klf4/KLF4	Konrad Hochedlinger	19764	pLV-tet0-Klf4	Klf4	<i>M. musculus</i>	mono	●	●	n/c	○	—	18371448	Stadtfeld et al., 2008a
Addgene	stem cell; Klf4/KLF4	Konrad Hochedlinger	19770	pAd-Klf4	Klf4	<i>M. musculus</i>	mono	●	●	n/c	○	—	18818365	Stadtfeld et al., 2008b
Addgene	stem cell; Klf4/KLF4	Konrad Hochedlinger	19777	FU-tet-o-hKLF4	KLF4	<i>H. sapiens</i>	mono	●	○	n/c	○	—	18786420	Maherali et al., 2008
Addgene	stem cell; Klf4/KLF4	Juan Belmonte	20074	pMSCV-Flag-hKlf4	hKlf4	<i>H. sapiens</i>	mono	●	○	○	—	—	18931654	Aasen et al., 2008
Addgene	stem cell; Klf4/KLF4	Rudolf Jaenisch	20322	Tet0-FUW-Klf4	Klf4	<i>M. musculus</i>	mono	●	●	○	○	—	18371436	Brambrink et al., 2008
Addgene	stem cell; Klf4/KLF4	Rudolf Jaenisch	20725	FUW-tet0-hKLF4	KLF4	<i>H. sapiens</i>	mono	●	●	○	○	—	18786421	Hockemeyer et al., 2008
Addgene	Klf4/KLF4	Rudolf Jaenisch	20727	FUW-tet0-lox-hKLF4	KLF4	<i>H. sapiens</i>	mono	●	●	○	○	—	19269371	Soldner et al., 2009
Addgene	Klf4/KLF4	Michel Sadelain	23243	pLM-mCherry-Klf4	mCherry_2A_KLF4	<i>H. sapiens</i>	mono	●	○	n/c	○	—	19549847	Papapetrou et al., 2009

(Continued on next page)





Table 1. Continued

Source				Construct Data				Form ^e		Sequence Validation			Publication	
Distribution ^a	Addgene Collection ^b	Depositing Scientist	Repository ID	Plasmid Name	Gene/Insert Name	Species ^c	Type ^d	Klf4 _S	Klf4 _L	AddGene ^f	Depositor	Direct ^g	PMID	Reference
Addgene	Klf4/KLF4	Rudolf Jaenisch	26274	pBRPyCAG-fmKlf4-DsRed-Ip	Klf4	<i>M. musculus</i>	mono	●		n/c	○	—	20442331	Hanna et al., 2010
Addgene	stem cell; Klf4/KLF4	Derrick Rossi	26815	pcDNA3.3_KLF4	5'UTR-KLF4-3'UTR	<i>H. sapiens</i>	mono	●		○	—	—	20888316	Warren et al., 2010
Addgene	stem cell; Klf4/KLF4	Steven Dowdy	36118	pCX4-KLF4	KLF4	<i>H. sapiens</i>	mono	n/d	n/d	n/c	—	—	22278060	Israel et al., 2012
Addgene	stem cell	Rudolf Jaenisch	20331	FUW-K0	Klf4-F2A-Oct4	<i>M. musculus</i>	bi		●	○	○	—	19109433	Carey et al., 2009
Addgene	stem cell	Rudolf Jaenisch	20332	FUW-KM	Klf4-F2A-cMyc	<i>M. musculus</i>	bi		●	○	○	—	19109433	Carey et al., 2009
Addgene	stem cell	James Thomson	21164	pSIN4-CMV-K2M	Klf4, cMyc	<i>H. sapiens</i>	bi	●		n/c	○	—	19325077	Yu et al., 2009
Addgene	stem cell	Shinya Yamanaka	27078	pCXLE-hSK	SOX2, KLF4	<i>H. sapiens</i>	bi	●		○	○	○	21460823	Okita et al., 2011
Addgene	stem cell; Klf4/KLF4	Shinya Yamanaka	41814	pCE-hSK	SOX2, KLF4	<i>H. sapiens</i>	bi	●		○	○	○	23193063	Okita et al., 2013
Addgene	Klf4/KLF4	Shinya Yamanaka	19771	pCX-OKS-2A	Oct3/4-2A-Klf4-2A-Sox2	<i>M. musculus</i>	poly	●		n/c	○	○	18845712	Okita et al., 2008
Addgene	stem cell; Klf4/KLF4	Rudolf Jaenisch	20321	Tet0-FUW-OSKM	Oct3/4-Sox2-Klf4-cMyc	<i>M. musculus</i>	poly		●	n/c	○	○	19109433	Carey et al., 2009
Addgene	stem cell; Klf4/KLF4	Rudolf Jaenisch	20325	FUW-SOKM	Sox2-P2A-Oct4-T2A-Klf4-E2A-cMyc	<i>M. musculus</i>	poly		●	n/c	○	—	19109433	Carey et al., 2009
Addgene	stem cell; Klf4/KLF4	Rudolf Jaenisch	20327	FUW-SOK	Sox2-F2A-Oct4-T2A-Klf4	<i>M. musculus</i>	poly		●	n/c	○	—	19109433	Carey et al., 2009
Addgene	stem cell	Rudolf Jaenisch	20328	FUW-OSKM	Oct4-P2A-Sox2-T2A-Klf4-E2A-cMyc	<i>M. musculus</i>	poly		●	n/c	○	—	19109433	Carey et al., 2009
Addgene	stem cell	Keisuke Kaji	20865	pCAGMKOSiE	c-Myc-F2A-Klf4-T2A-Oct4-E2A-Sox2 (Alt name)	<i>M. musculus</i>	poly		●	○	○	○	19252477	Kaji et al., 2009

(Continued on next page)

Please cite this article in press as: Kim et al., KLF4-N-Terminal Variance Modulates Induced Reprogramming to Pluripotency, Stem Cell Reports (2015), <http://dx.doi.org/10.1016/j.stemcr.2015.02.004>

Table 1. Continued

Source				Construct Data				Form ^e		Sequence Validation			Publication		
	Distribution ^a	Addgene Collection ^b	Depositing Scientist	Repository ID	Plasmid Name	Gene/Insert Name	Species ^c	Type ^d	Klf4 _S	Klf4 _L	AddGene ^f	Depositor	Direct ^g	PMID	Reference
Addgene	stem cell		Keisuke Kaji	20866	pCAG2LMKOSim0	c-Myc-F2A-Klf4-T2A-Oct4-E2A-Sox2-ires-mOrange	<i>M. musculus</i>	poly	●	○	○	○	○	19252477	Kaji et al., 2009
Addgene	stem cell; Klf4/KLF4		James Thomson	20923	pEP4 E02S EM2K	Oct4 and Sox2; Myc and Klf4	<i>H. sapiens</i>	poly	●		n/c	○	—	19325077	Yu et al., 2009
Addgene	stem cell		James Thomson	20924	pEP4 E02S CK2M EN2L	Oct4 and Sox2; Nanog and Lin28; Klf4 and Myc	<i>H. sapiens</i>	poly	●		n/c	○	—	19325077	Yu et al., 2009
Addgene	stem cell		James Thomson	20925	pEP4 E02S EN2K	Oct4 and Sox2; Nanog and Klf4	<i>H. sapiens</i>	poly	●		n/c	○	—	19325077	Yu et al., 2009
Addgene	stem cell; Klf4/KLF4		James Thomson	20927	pEP4 E02S ET2K	Oct4 and Sox2; SV40LT and Klf4	<i>H. sapiens</i>	poly	●		n/c	○	—	19325077	Yu et al., 2009
Addgene	stem cell		Tim Townes	21627	pKP332 (Lenti-OSK1)	hOCT4 - 2A - hSOX2 - 2A - hKLF4	<i>H. sapiens</i>	poly	●		○	○	—	19415770	Chang et al., 2009
Addgene	stem cell; Klf4/KLF4		Jose Cibelli	24603	OKSIM	Oct4 KLF4 Sox2 c-Myc	<i>H. sapiens</i>	poly	●		n/c	○	—	20030562	Ross et al., 2010
Addgene	—		Michel Sadelain	27512	pLM-fSV2A	OCT4_T2A_KLF4_P2A_cMYC_E2A_SOX2	<i>H. sapiens</i>	poly	●		—	○	—	21151124	Papapetrou et al., 2011
Addgene	stem cell		Linzhao Cheng	28213	pEB-C5	Oct4, Sox2, Klf4, c-Myc, Lin28	<i>M. musculus</i>	poly	●		○	○	—	21243013	Chou et al., 2011
Kotton Lab	—		Darrell Kotton, Gustavo Mostoslavsky	—	pHAGE-Tet-STEMCCA	Oct3/4-Klf4-ires-Sox2-cMyc	<i>M. musculus</i>	poly	●		—	—	○	19096035	Sommer et al., 2009
WTSI	—		Alan Bradley	—	pPB-CAG.OSKM-puΔtk	0-T2A-S-T2A-K-F2A-M	<i>M. musculus</i>	poly	●		—	○	—	19337237	Yusa et al., 2009
RIKEN BRC	—		Knut Woltjen	RDB13133	PB-TAC-OKMS	Oct3/4-Klf4-cMyc-Sox2	<i>M. musculus</i>	poly	●		—	—	○		this study
RIKEN BRC	—		Knut Woltjen	RDB13132	PB-TAC-OSKM	Oct3/4-Sox2-Klf4-cMyc (from 20321)	<i>M. musculus</i>	poly	●		—	—	○		this study

(Continued on next page)





Table 1. Continued

Source	Construct Data			Form ^e		Sequence Validation			Publication						
	Distribution ^a	Addgene Collection ^b	Depositing Scientist	Repository ID	Plasmid Name	Gene/Insert Name	Species ^c	Type ^d	Klf4 _S	Klf4 _L	AddGene ^f	Depositor	Direct ^g	PMID	Reference
RIKEN BRC	—	—	Knut Woltjen	RDB13135	PB-TAC-OK+9MS	Oct3/4-Klf4+9-cMyc-Sox2	<i>M. musculus</i>	poly	●	—	—	—	○	—	this study
RIKEN BRC	—	—	Knut Woltjen	RDB13136	PB-TAC-STEMCCA	Oct3/4-Klf4-ires-Sox2-cMyc (from Sommer et al., 2009)	<i>M. musculus</i>	poly	●	—	—	—	○	—	this study
RIKEN BRC	—	—	Knut Woltjen	RDB13134	PB-TAC-MKOS	c-Myc-F2A-Klf4-T2A-Oct4-E2A-Sox2 (from 20866)	<i>M. musculus</i>	poly	●	—	—	—	○	—	this study
RIKEN BRC	—	—	Knut Woltjen	RDB13137	PB-TAC-EB-C5	Oct4, Sox2, Klf4, c-Myc, Lin28 (from 28213)	<i>M. musculus</i>	poly	●	—	—	—	○	—	this study
RIKEN BRC	—	—	Knut Woltjen	RDB13138	PB-TAC-WTSI	0-T2A-S-T2A-K-F2A-M (from Yusa et al., 2009)	<i>M. musculus</i>	poly	●	—	—	—	○	—	this study

WTSI, Wellcome Trust Sanger Institute; RIKEN BRC, RIKEN Bio Resource Center DNA Bank. Closed circles indicate the Klf4 variant, and open circles denote sequence validation steps for each construct. See also Figures 3 and S3.

^aOnly vectors containing Klf4 are listed. Data from Addgene were current as of September 3, 2014. As Addgene is an independently curated and dynamically changing database, the authors do not warrant the accuracy or completeness of this resource beyond the date of data collection.

^bAddgene Collection lists can be found at <http://www.addgene.org/stemcell/> and <http://www.addgene.org/KLF/> or by browsing for Klf4 (gene 16600) or KLF4 (gene 9314).

^cCompared to mouse Klf4_L, the human ORF is 87% and 90% similar at the nucleotide and amino acid levels, respectively, with 100% conservation across the first 35 amino acids. The effect of human Klf4_{S/L} on reprogramming was not tested in this study.

^d“Type” refers to the number of cistrons or ORFs in the construct.

^eComparison of the ATG start site with U70662.1 (Klf4_S) and U20344.1 (Klf4_L) reference cDNAs. Note that for polycistronic vectors, this annotation does not take into account elongation by 2A peptides. n/d, form not determined by the available data.

^fValidation of Klf4 identity was from Addgene sequencing data. n/c, no coverage of the Klf4 start site, although available sequence confirmed the presence of Klf4.

^gCassette sequences were verified empirically by the authors.



variants have seen unprejudiced use among vectors constructed for reprogramming (Table 1 and associated references). OKMS (*Klf4_S*) presented low KLF4 levels, which were restored along with *Klf4_L*-related phenotypes by elongation of the KLF4_S N terminus by 9aa. Thus, OK⁺MS excluded the influence of 2A peptide choice and factor order variation. Moreover, high KLF4-associated phenotypes were reproduced by supplementation of OKMS with either monocistronic *Klf4_S* or *Klf4_L*, limiting the effect to a polycistronic context. Relative stoichiometry was explored in a recent study, and it was found that chemically controlled degradation of KLF4 resulted in premature termination of reprogramming (Nishimura et al., 2014). Although precise factor titration and more direct biochemical assays may be required, our monocistronic reprogramming data argue against modification of an N-terminal functional domain, and rather support the idea that threshold levels of KLF4 are important for minimizing the occurrence of partial reprogramming.

Polycistronic cassettes encoding KLF4_S tend to permit rapid expansion of transgenic cells with robust SSEA-1 activation. Yet, this majority population is ultimately impeded in the acquisition and stabilization of pluripotency, as indicated by transgene dependence and high-level expression of markers associated with pre-iPSCs (Mikkelsen et al., 2008; Theunissen et al., 2011). Polycistronic reprogramming with *Klf4_L* or OKMS supplementation with *Klf4_{S/L}* improved reporter activation and dox independence. Nanog-GFP reporter activation is consistent with a central role for KLF4 in the core ESC pluripotency network, as ectopic expression of *Klf4* promotes epiblast stem cell conversion to ground-state pluripotency (Guo et al., 2009) and prevents loss of pluripotency in the absence of LIF (Niwa et al., 2009). Transgene silencing is considered a hallmark of complete reprogramming (Golipour et al., 2012). How the silencing phenomenon is related to the acquisition of pluripotency, and whether it is coordinated directly or indirectly through KLF4 are issues of considerable interest.

Individual expression of either *Klf4_S* or *Klf4_L* in MEFs led to a potent epidermal gene response (Figure S2B). Moreover, a similar response was noted as a common feature of d6 reprogramming populations induced with *Klf4_L* cassettes (Figure 3B). A retrospective examination of early reprogramming experiments recalls reports of epidermis-related gene activation (Mikkelsen et al., 2008). *Klf4* knockout mice die postnatally from failed epidermal stratification (Segre et al., 1999). Reciprocally, ectopic *Klf4* expression during embryogenesis results in premature barrier formation (Jaubert et al., 2003). Therefore, it is pertinent that high KLF4 stoichiometry induces a cascade of epithelialization and expression of epidermis-associated genes such as *Krt6a*, *Krt17*, *Spr1a*, *Cnfn*, and *Tgm1* during

early reprogramming (Figures 3A and 3B; Table S1). Interestingly, many of these genes are not expressed in ESCs, nor are they maintained in GFP⁺ iPSCs (data not shown), which brings into question their relevance in iPSC derivation. To address potential cellular heterogeneity, it will be important to link gene expression responses and reprogramming outcomes to specific subpopulations of cells. Thus, it remains to be determined whether the epidermal response elicited by excess KLF4 in the early phase directly contributes to high-fidelity reprogramming or to an alternate cell fate.

On the path toward induced pluripotency, investigators rely on gene expression patterns as milestones to gauge appropriate progression, and comparative analysis of publically available gene expression profiles is a common approach. Clearly, our data show that inconsistencies in the relative levels of KLF4 to OCT3/4, SOX2, and c-MYC can fundamentally confound comparative analysis. Application of monocistronic *Klf4_S* or *Klf4_L* leads to nearly indistinguishable reprogramming phenotypes. Thus, typical clonal isolation of fully reprogrammed iPSCs with monocistronic vectors, which is subject to phenotypic selection for appropriate factor expression levels, should be mostly unaffected. Mechanistic studies, on the other hand, are prone to transcriptional noise arising from variable factor expression between cells and among transgenes. We expect the KLF4 threshold effects observed herein to be pronounced when the relative factor stoichiometry is fixed, for polycistronic transfection or even in secondary reprogramming systems with pre-integrated transgenes (Wernig et al., 2008; Woltjen et al., 2009). As such, we must be mindful that it is difficult to make direct comparisons across distinct reprogramming systems without first defining the inherent factor stoichiometry.

EXPERIMENTAL PROCEDURES

Plasmid Construction

The PB transposon-based PB-TAC expression vector (RDB13131) was generated by standard cloning (restriction digestion and ligation). PB-TAB vectors containing the four Yamanaka factors were generated by Gateway Cloning (Invitrogen) as described previously (Woltjen et al., 2009). Monocistronic and polycistronic reprogramming cassettes constructed in-house or obtained from public resources (Table 1) were cloned into pDONR221 using PCR and attB/P Clonase (Invitrogen) or pENTR2B using standard restriction endonuclease cloning or InFusion (Takara Clontech). Note that the cassette from pPB-CAG.OSKMBpuΔtk (Yusa et al., 2009) is in the order O-S-K-M, similarly to OSKM (Carey et al., 2009), and thus is referred to in the text as WTSI to avoid confusion. Modifications such as N-terminal extension and HA tagging were produced using InFusion or the Q5 Site-Directed Mutagenesis Kit (New England Biolabs). Sequences of the main Gateway

Entry constructs (from *attL1* to *attL2*) were obtained using Sanger sequencing with Big Dye Terminator Ver3.1 chemistry (ABI) and assembled as contigs using Sequencher (GeneCodes). Complete details regarding the cloning procedures used, including InFusion amplification and sequencing primers, are available upon request.

MEF Isolation

Nanog-GFP (Okita et al., 2007) transgenic reporter mice were maintained as homozygotes on a C57BL/6 background. For ROSA-rtTA; Nanog-GFP double transgenic MEFs, C57BL/6 homozygous ROSA26-rtTA females (Ohnishi et al., 2014) and inbred homozygous Nanog-GFP males were crossed. Mice bearing *Col1a1*-targeted OSKM and OKMS cassettes were generated as described previously (Ohnishi et al., 2014). MEFs were isolated from 12.5–13.5 days postcoitum transgenic embryos. Embryos were decapitated, eviscerated, and macerated, and then dissociated with 0.25% trypsin/EDTA at 37°C for 15 min and plated in DMEM containing 10% fetal bovine serum (FBS), penicillin-streptomycin, and L-glutamine. The presence of the desired transgenes and male gender were determined by PCR genotyping of residual embryonic tissues. Cells from male embryos were expanded 1:5 once and then frozen in liquid nitrogen. Cells for reprogramming were defrosted, counted, and plated for transfection without additional expansion. The genotyping primers are available upon request. Animal care and experiments using animal tissues were approved by the CiRA Animal Experiment Committee in accordance with Kyoto University guidelines.

PB Reprogramming and iPSC and ESC Culture

MEFs were seeded in DMEM containing 10% FBS, penicillin-streptomycin, and L-glutamine on gelatinized (0.1%) 6-well dishes at a density of 1.0×10^5 cells per 10 cm^2 . After a 24 hr culture, FugeneHD (Promega) was used to transfect cells with 500 ng of transposons (PB-TAC-OSKM, -OKMS, -OK⁺MS, -MKOS, -STEMCCA, -EB-C5, -WT5I, -OK_{N-HA}MS, -OK⁺_{N-HA}MS, and -lacZ) plus 1,000 ng of pCyL43 PB transposase plasmid at a Fugene/DNA ratio of 8 μL :2 μg . For top-up experiments, cells were co-transfected with 500 ng of PB-TAC-OKMS along with 500 ng of PB-TAB-*Oct3/4*, -*Sox2*, -*c-Myc*, -*Klf4s*, or -*Klf4L*, plus 1,000 ng of pCyL43 PB transposase plasmid. After 24 hr, the medium was replaced with ESC medium (DMEM containing 15% FBS, penicillin-streptomycin, GlutaMAX, β -mercaptoethanol, sodium-pyruvate, non-essential amino acids, LIF, and dox [1 $\mu\text{g}/\text{mL}$]). After transfection, cells were fed daily with dox-containing ESC medium. On d8, cells were trypsinized and re-seeded at 3.0×10^5 cells per 10 cm^2 on gelatin for late-stage analysis (until d18). For dox withdrawal, cells were again harvested on d18 and re-seeded at 3.0×10^5 cells per 10 cm^2 on gelatin in the presence or absence of dox, and analyzed on d24. For isolation of factor-independent iPSC clones, d18 cultures were reseeded on gelatin at limiting dilutions in the absence of dox, and colonies were picked on d24. Southern blot analysis using *HindIII* digestion and an mCherry probe identified genetically unique iPSC lines. Both dox-independent iPSCs and ESCs were maintained on mitomycin-c-inactivated DR4 MEF feeders and gelatin in ESC medium, with passage every 2–3 days. For all

cells, total viable cell counts were performed using a TC10 Automated Cell Counter (Bio-Rad) with trypan blue exclusion.

HEK293T Cell Culture and PB Transfection

HEK293T cells were maintained in DMEM containing 10% FBS, penicillin-streptomycin, and L-glutamine. Then 3.0×10^5 cells per 10 cm^2 were transfected with 500 ng of transposons (PB-TAC-OK_{N/C-HA}MS and -OK⁺_{N/C-HA}MS) plus 500 ng of PB-CAG-rtTA (Woltjen et al., 2009) at a Fugene/DNA ratio of 8 μL :2 μg . After 24 hr, the culture medium was replaced with medium containing dox (1 $\mu\text{g}/\text{mL}$). After an additional 24 hr, transfected cells were harvested for western blot analysis.

Whole-Well Fluorescence Microscopy Imaging

Mouse fibroblasts were plated on standard tissue culture 6-well plastic plates (BD Falcon Labware). Images were acquired with a Nikon BioStation CT (Nikon) equipped with GFP and mCherry fluorescence filters and phase contrast using 2 \times lenses. The single-plane images of each channel were stitched automatically using the automated image analysis software CL-Quant 3.0 (Nikon).

AP Staining

Staining for AP activity was performed using the BCIP/NBT Alkaline Phosphatase Substrate Kit IV (SK-5400, Vector Laboratories) according to the manufacturer's instructions. Images were acquired with a color camera (Canon IXY Digital 900IS), and colony count analysis was performed using a custom CL-Quant 3.0 macro developed in cooperation with Nikon, with AP-stained, mock-transfected MEF plates used to establish background.

Flow Cytometry and Cell Sorting

For FACS analysis, 3.0×10^5 cells were stained on ice for 30 min with Alexa Fluor 647 conjugated SSEA-1 (480, sc-21702, Santa Cruz Biotechnology) antibody or the corresponding isotype-matched control, mouse IgM (1:50 dilution). Control staining with the appropriate isotype-matched control monoclonal antibodies (BD Biosciences) was included to establish thresholds for positive staining. Samples were analyzed using a BD LSRFortessa Cell Analyzer (BD Biosciences) with BD FACSDiva software (BD Biosciences). Flow cytometry data were analyzed and generated by FlowJo software (Tree Star). For cell sorting, the mCherry⁺ cell population was collected on a BD FACSAria II cell sorter (BD Biosciences).

Microarray Analysis

Total RNA was prepared from harvested cells using the RNeasy Mini Kit (QIAGEN) according to the manufacturer's instructions. cDNA synthesis and transcriptional amplification were performed using 200 ng of total RNA with the Whole Transcript (WT) Expression Kit (Ambion/Affymetrix). Fragmented and biotin-labeled cDNA targets were hybridized to GeneChip Mouse Gene 1.0 ST arrays (Affymetrix) according to the manufacturer's protocols. Hybridized arrays were scanned using an Affymetrix GeneChip Scanner. Probe signal intensities were normalized with the RMA algorithm in GeneSpring. Quality, correlation, and cluster analyses were performed using GeneSpring GX software v12.1 (Agilent



Technologies). GO term analysis was performed using the NIH DAVID Bioinformatics tool (<http://david.abcc.ncifcrf.gov/>). There is no straightforward way to derive gene numbers directly from probe sets, as the Affymetrix GeneChip Array platform makes use of redundant probes for a small subset of genes. Moreover, each expressed sequence tag (EST) is represented by a unique probe, despite the fact that multiple ESTs may be associated with a single gene transcript. For clarity, we refer to probe sets or entities as “genes” in the text.

Protein Analysis

For western analysis, we prepared total cell lysates by boiling 1×10^6 cells for 10 min in SDS sample buffer (25 mM Tris (pH 6.8), 2% β -mercaptoethanol, 3% SDS, 0.05% bromophenol blue, and 5% glycerol). Lysates were resolved on SDS-polyacrylamide gels, and proteins were detected by western blotting using ECL Plus (Amersham Pharmacia). For western analysis, Sox-2 (Y-17, sc-17320, 1:1,000) and GKLF (H-180, sc-20691, 1:500) antibodies were used as described previously (Kaji et al., 2009). Mouse Anti-Oct-3/4 (40/Oct-3, 611203, 1:1,000) and c-Myc (9402, 1:1,000) antibodies were obtained from BD Biosciences and Cell Signaling, respectively. HA-probe (F-7, sc-7392, 1:200) and anti-actin (A2066, 1:5,000) antibodies were obtained from Santa Cruz Biotechnology and Sigma-Aldrich, respectively.

Material Distribution

The PB-TAC reprogramming transposons are available through the RIKEN BRC DNA Bank (<http://dna.brc.riken.jp>) under accession numbers RDB13131–RDB13138. Gateway versions of the polycistronic reprogramming cassettes will be made available through AddGene (<http://www.addgene.org>). The PB transposase vector pCyL43 is available through the Wellcome Trust Sanger Center (http://www.sanger.ac.uk/form/Sanger_CloneRequests).

ACCESSION NUMBERS

Datasets for the d6 gene expression microarray analysis have been deposited in the Gene Expression Omnibus under accession number GSE65468.

SUPPLEMENTAL INFORMATION

Supplemental Information includes Supplemental Experimental Procedures, three figures, and one table and can be found with this article online at <http://dx.doi.org/10.1016/j.stemcr.2015.02.004>.

AUTHOR CONTRIBUTIONS

K.W. conceived the study and wrote the manuscript with S.-I.K. S.-I.K., F.O.-Y., and K.W. designed experiments. K.W. and R.H. performed initial reprogramming trials, and S.-I.K. performed all subsequent reprogramming experiments. K.W. designed and R.H. generated and sequenced plasmid constructs. S.-I.K. collected and analyzed FACS data. F.O.-Y. and S.-I.K. collected and analyzed protein and imaging data. S.-I.K. and S.L. performed bioinformatic analyses with advice from T.Y. K.O. and Y.Y. provided reporter cell lines and mice. Y.Y. and S.Y. provided critical input on experimental design and data analysis.

ACKNOWLEDGMENTS

We thank Kazutoshi Takahashi, Masamitsu Sone, and Ren Shimamoto for their critical readings of the manuscript, and Katsunori Semi for bioinformatics advice. We also thank Chiho Sakurai, Michiko Nakamura, and Akiko Oishi for technical support; Toshiko Sato for microarray preparations; Akito Tanaka for blastocyst injections; and Kanako Asano and Kotaro Ohnishi for mouse husbandry. We appreciate the advice of Hiroaki Kii (Nikon, Japan) regarding image acquisition and analysis. We also thank Darrell N. Kotton and Gustavo Mostoslavsky (Boston University School of Medicine) for providing pHAGE-Tet-STEMCCA, Alan Bradley and Kosuke Yusa (Wellcome Trust Sanger Institute) for providing pPB-CAG.OSKMBpu Δ tk, Hitoshi Niwa (RIKEN Center for Developmental Biology) for providing the p*Lefty1*-luc reporter, and all Addgene contributors, especially Linzhao Cheng and Rudolf Jaenisch. This work was supported by the Cabinet Office, Government of Japan and the Japan Society for the Promotion of Science (JSPS) through the Funding Program for World-Leading Innovative R&D on Science and Technology (FIRST Program), the Core Center for iPS Cell Research, the Research Center Network for Realization of Regenerative Medicine, and the Strategic International Collaborative Research Program of the Japan Science and Technology Agency (JST). K.W. is a Hakubi Center Special Project Researcher. S.Y. is a non-salaried scientific advisor of iPS Academia Japan. S.L. received funding from EPASI (JSPS/National Science Foundation, 2013). S.-I.K. is a JSPS Fellowship recipient (2011–2013) and JST Researcher.

Received: August 8, 2014

Revised: February 6, 2015

Accepted: February 6, 2015

Published: March 12, 2015

REFERENCES

- Aasen, T., Raya, A., Barrero, M.J., Garreta, E., Consiglio, A., Gonzalez, F., Vassena, R., Bilic, J., Pekarik, V., Tiscornia, G., et al. (2008). Efficient and rapid generation of induced pluripotent stem cells from human keratinocytes. *Nat. Biotechnol.* *26*, 1276–1284.
- Blelloch, R., Venere, M., Yen, J., and Ramalho-Santos, M. (2007). Generation of induced pluripotent stem cells in the absence of drug selection. *Cell Stem Cell* *1*, 245–247.
- Brambrink, T., Foreman, R., Welstead, G.G., Lengner, C.J., Wernig, M., Suh, H., and Jaenisch, R. (2008). Sequential expression of pluripotency markers during direct reprogramming of mouse somatic cells. *Cell Stem Cell* *2*, 151–159.
- Carey, B.W., Markoulaki, S., Hanna, J., Saha, K., Gao, Q., Mitalipova, M., and Jaenisch, R. (2009). Reprogramming of murine and human somatic cells using a single polycistronic vector. *Proc. Natl. Acad. Sci. USA* *106*, 157–162.
- Carey, B.W., Markoulaki, S., Hanna, J.H., Faddah, D.A., Buganim, Y., Kim, J., Ganz, K., Steine, E.J., Cassady, J.P., Creighton, M.P., et al. (2011). Reprogramming factor stoichiometry influences the epigenetic state and biological properties of induced pluripotent stem cells. *Cell Stem Cell* *9*, 588–598.



- Chang, C.W., Lai, Y.S., Pawlik, K.M., Liu, K., Sun, C.W., Li, C., Schoeb, T.R., and Townes, T.M. (2009). Polycistronic lentiviral vector for “hit and run” reprogramming of adult skin fibroblasts to induced pluripotent stem cells. *Stem Cells* 27, 1042–1049.
- Chou, B.K., Mali, P., Huang, X., Ye, Z., Dowey, S.N., Resar, L.M., Zou, C., Zhang, Y.A., Tong, J., and Cheng, L. (2011). Efficient human iPS cell derivation by a non-integrating plasmid from blood cells with unique epigenetic and gene expression signatures. *Cell Res.* 21, 518–529.
- David, L., and Polo, J.M. (2014). Phases of reprogramming. *Stem Cell Res. (Amst.)* 12, 754–761.
- Garrett-Sinha, L.A., Eberspaecher, H., Seldin, M.F., and de Crombrughe, B. (1996). A gene for a novel zinc-finger protein expressed in differentiated epithelial cells and transiently in certain mesenchymal cells. *J. Biol. Chem.* 271, 31384–31390.
- Golipour, A., David, L., Liu, Y., Jayakumaran, G., Hirsch, C.L., Trcka, D., and Wrana, J.L. (2012). A late transition in somatic cell reprogramming requires regulators distinct from the pluripotency network. *Cell Stem Cell* 11, 769–782.
- Graf, T. (2011). Historical origins of transdifferentiation and reprogramming. *Cell Stem Cell* 9, 504–516.
- Guo, G., Yang, J., Nichols, J., Hall, J.S., Eyres, I., Mansfield, W., and Smith, A. (2009). Klf4 reverts developmentally programmed restriction of ground state pluripotency. *Development* 136, 1063–1069.
- Hanna, J., Cheng, A.W., Saha, K., Kim, J., Lengner, C.J., Soldner, F., Cassady, J.P., Muffat, J., Carey, B.W., and Jaenisch, R. (2010). Human embryonic stem cells with biological and epigenetic characteristics similar to those of mouse ESCs. *Proc. Natl. Acad. Sci. USA* 107, 9222–9227.
- Hockemeyer, D., Soldner, F., Cook, E.G., Gao, Q., Mitalipova, M., and Jaenisch, R. (2008). A drug-inducible system for direct reprogramming of human somatic cells to pluripotency. *Cell Stem Cell* 3, 346–353.
- Israel, M.A., Yuan, S.H., Bardy, C., Reyna, S.M., Mu, Y., Herrera, C., Hefferan, M.P., Van Gorp, S., Nazor, K.L., Boscolo, F.S., et al. (2012). Probing sporadic and familial Alzheimer’s disease using induced pluripotent stem cells. *Nature* 482, 216–220.
- Jaubert, J., Cheng, J., and Segre, J.A. (2003). Ectopic expression of kruppel like factor 4 (Klf4) accelerates formation of the epidermal permeability barrier. *Development* 130, 2767–2777.
- Kaji, K., Norrby, K., Paca, A., Mileikovsky, M., Mohseni, P., and Woltjen, K. (2009). Virus-free induction of pluripotency and subsequent excision of reprogramming factors. *Nature* 458, 771–775.
- Lowry, W.E., Richter, L., Yachechko, R., Pyle, A.D., Tchieu, J., Sridharan, R., Clark, A.T., and Plath, K. (2008). Generation of human induced pluripotent stem cells from dermal fibroblasts. *Proc. Natl. Acad. Sci. USA* 105, 2883–2888.
- Maherali, N., Ahfeldt, T., Rigamonti, A., Utikal, J., Cowan, C., and Hochedlinger, K. (2008). A high-efficiency system for the generation and study of human induced pluripotent stem cells. *Cell Stem Cell* 3, 340–345.
- Mikkelsen, T.S., Hanna, J., Zhang, X., Ku, M., Wernig, M., Schorderet, P., Bernstein, B.E., Jaenisch, R., Lander, E.S., and Meissner, A. (2008). Dissecting direct reprogramming through integrative genomic analysis. *Nature* 454, 49–55.
- Nakatake, Y., Fukui, N., Iwamatsu, Y., Masui, S., Takahashi, K., Yagi, R., Yagi, K., Miyazaki, J., Matoba, R., Ko, M.S., and Niwa, H. (2006). Klf4 cooperates with Oct3/4 and Sox2 to activate the Lefty1 core promoter in embryonic stem cells. *Mol. Cell. Biol.* 26, 7772–7782.
- Nishimura, K., Kato, T., Chen, C., Oinam, L., Shiomitsu, E., Ayakawa, D., Ohtaka, M., Fukuda, A., Nakanishi, M., and Hisatake, K. (2014). Manipulation of KLF4 expression generates iPSCs paused at successive stages of reprogramming. *Stem Cell Reports* 3, 915–929.
- Niwa, H., Ogawa, K., Shimosato, D., and Adachi, K. (2009). A parallel circuit of LIF signalling pathways maintains pluripotency of mouse ES cells. *Nature* 460, 118–122.
- Ohnishi, K., Semi, K., Yamamoto, T., Shimizu, M., Tanaka, A., Mitsunaga, K., Okita, K., Osafune, K., Arioka, Y., Maeda, T., et al. (2014). Premature termination of reprogramming in vivo leads to cancer development through altered epigenetic regulation. *Cell* 156, 663–677.
- Okita, K., Ichisaka, T., and Yamanaka, S. (2007). Generation of germline-competent induced pluripotent stem cells. *Nature* 448, 313–317.
- Okita, K., Nakagawa, M., Hyenjong, H., Ichisaka, T., and Yamanaka, S. (2008). Generation of mouse induced pluripotent stem cells without viral vectors. *Science* 322, 949–953.
- Okita, K., Matsumura, Y., Sato, Y., Okada, A., Morizane, A., Okamoto, S., Hong, H., Nakagawa, M., Tanabe, K., Tezuka, K., et al. (2011). A more efficient method to generate integration-free human iPSCs. *Nat. Methods* 8, 409–412.
- Okita, K., Yamakawa, T., Matsumura, Y., Sato, Y., Amano, N., Watanabe, A., Goshima, N., and Yamanaka, S. (2013). An efficient nonviral method to generate integration-free human-induced pluripotent stem cells from cord blood and peripheral blood cells. *Stem Cells* 31, 458–466.
- O’Malley, J., Skylaki, S., Iwabuchi, K.A., Chantzoura, E., Ruetz, T., Johnsson, A., Tomlinson, S.R., Linnarsson, S., and Kaji, K. (2013). High-resolution analysis with novel cell-surface markers identifies routes to iPSC cells. *Nature* 499, 88–91.
- Papapetrou, E.P., Tomishima, M.J., Chambers, S.M., Mica, Y., Reed, E., Menon, J., Tabar, V., Mo, Q., Studer, L., and Sadelain, M. (2009). Stoichiometric and temporal requirements of Oct4, Sox2, Klf4, and c-Myc expression for efficient human iPSC induction and differentiation. *Proc. Natl. Acad. Sci. USA* 106, 12759–12764.
- Papapetrou, E.P., Lee, G., Malani, N., Setty, M., Riviere, I., Tirunagari, L.M., Kadota, K., Roth, S.L., Giardina, P., Viale, A., et al. (2011). Genomic safe harbors permit high beta-globin transgene expression in thalassemia induced pluripotent stem cells. *Nat. Biotechnol.* 29, 73–78.
- Park, I.H., Zhao, R., West, J.A., Yabuuchi, A., Huo, H., Ince, T.A., Lerou, P.H., Lensch, M.W., and Daley, G.Q. (2008). Reprogramming of human somatic cells to pluripotency with defined factors. *Nature* 451, 141–146.



- Plath, K., and Lowry, W.E. (2011). Progress in understanding reprogramming to the induced pluripotent state. *Nat. Rev. Genet.* *12*, 253–265.
- Polo, J.M., Anderssen, E., Walsh, R.M., Schwarz, B.A., Nefzger, C.M., Lim, S.M., Borkent, M., Apostolou, E., Alaei, S., Cloutier, J., et al. (2012). A molecular roadmap of reprogramming somatic cells into iPS cells. *Cell* *151*, 1617–1632.
- Ross, P.J., Suhr, S.T., Rodriguez, R.M., Chang, E.A., Wang, K., Siripattarapivat, K., Ko, T., and Cibelli, J.B. (2010). Human-induced pluripotent stem cells produced under xeno-free conditions. *Stem Cells Dev.* *19*, 1221–1229.
- Samavarchi-Tehrani, P., Golipour, A., David, L., Sung, H.K., Beyer, T.A., Datti, A., Woltjen, K., Nagy, A., and Wrana, J.L. (2010). Functional genomics reveals a BMP-driven mesenchymal-to-epithelial transition in the initiation of somatic cell reprogramming. *Cell Stem Cell* *7*, 64–77.
- Segre, J.A., Bauer, C., and Fuchs, E. (1999). Klf4 is a transcription factor required for establishing the barrier function of the skin. *Nat. Genet.* *22*, 356–360.
- Shields, J.M., Christy, R.J., and Yang, V.W. (1996). Identification and characterization of a gene encoding a gut-enriched Krüppel-like factor expressed during growth arrest. *J. Biol. Chem.* *271*, 20009–20017.
- Soldner, F., Hockemeyer, D., Beard, C., Gao, Q., Bell, G.W., Cook, E.G., Hargus, G., Blak, A., Cooper, O., Mitalipova, M., et al. (2009). Parkinson's disease patient-derived induced pluripotent stem cells free of viral reprogramming factors. *Cell* *136*, 964–977.
- Sommer, C.A., Stadtfeld, M., Murphy, G.J., Hochedlinger, K., Kotton, D.N., and Mostoslavsky, G. (2009). Induced pluripotent stem cell generation using a single lentiviral stem cell cassette. *Stem Cells* *27*, 543–549.
- Stadtfeld, M., Maherali, N., Breault, D.T., and Hochedlinger, K. (2008a). Defining molecular cornerstones during fibroblast to iPS cell reprogramming in mouse. *Cell Stem Cell* *2*, 230–240.
- Stadtfeld, M., Nagaya, M., Utikal, J., Weir, G., and Hochedlinger, K. (2008b). Induced pluripotent stem cells generated without viral integration. *Science* *322*, 945–949.
- Takahashi, K., and Yamanaka, S. (2006). Induction of pluripotent stem cells from mouse embryonic and adult fibroblast cultures by defined factors. *Cell* *126*, 663–676.
- Takahashi, K., Tanabe, K., Ohnuki, M., Narita, M., Ichisaka, T., Tomoda, K., and Yamanaka, S. (2007). Induction of pluripotent stem cells from adult human fibroblasts by defined factors. *Cell* *131*, 861–872.
- Theunissen, T.W., and Jaenisch, R. (2014). Molecular control of induced pluripotency. *Cell Stem Cell* *14*, 720–734.
- Theunissen, T.W., van Oosten, A.L., Castelo-Branco, G., Hall, J., Smith, A., and Silva, J.C. (2011). Nanog overcomes reprogramming barriers and induces pluripotency in minimal conditions. *Curr. Biol.* *21*, 65–71.
- Warren, L., Manos, P.D., Ahfeldt, T., Loh, Y.H., Li, H., Lau, F., Ebina, W., Mandal, P.K., Smith, Z.D., Meissner, A., et al. (2010). Highly efficient reprogramming to pluripotency and directed differentiation of human cells with synthetic modified mRNA. *Cell Stem Cell* *7*, 618–630.
- Wernig, M., Lengner, C.J., Hanna, J., Lodato, M.A., Steine, E., Foreman, R., Staerk, J., Markoulaki, S., and Jaenisch, R. (2008). A drug-inducible transgenic system for direct reprogramming of multiple somatic cell types. *Nat. Biotechnol.* *26*, 916–924.
- Woltjen, K., Michael, I.P., Mohseni, P., Desai, R., Mileikovsky, M., Hämmäläinen, R., Cowling, R., Wang, W., Liu, P., Gertsenstein, M., et al. (2009). piggyBac transposition reprograms fibroblasts to induced pluripotent stem cells. *Nature* *458*, 766–770.
- Yamaguchi, S., Hirano, K., Nagata, S., and Tada, T. (2011). Sox2 expression effects on direct reprogramming efficiency as determined by alternative somatic cell fate. *Stem Cell Res. (Amst.)* *6*, 177–186.
- Yu, J., Hu, K., Smuga-Otto, K., Tian, S., Stewart, R., Slukvin, I.I., and Thomson, J.A. (2009). Human induced pluripotent stem cells free of vector and transgene sequences. *Science* *324*, 797–801.
- Yusa, K., Rad, R., Takeda, J., and Bradley, A. (2009). Generation of transgene-free induced pluripotent mouse stem cells by the piggyBac transposon. *Nat. Methods* *6*, 363–369.